Reduction of Nicotinamides, Flavins, and Manganese Porphyrins by Formate, Catalyzed by Membrane-Bound Rhodium Complexes

J. H. van Esch, M. A. M. Hoffmann, and R. J. M. Nolte*

Laboratorium of Organic Chemistry, Nijmegen SON Research Center, Toernooiveld, 6525 ED Nijmegen, The Netherlands

Received April 5, 1994 (Revised Manuscript Received December 13, 1994®)

Two polymerizable cyclopentadienyl-2,2′-bipyridinerhodium complexes and one amphiphilic rhodium complex have been synthesized and incorporated into the bilayers of vesicles formed from a polymerizable ammonium surfactant. Incorporation was achieved by chemical linkage (via a copolymerization reaction) or by physical absorption. The complexes are located at different positions in the bilayer, viz. in the hydrophobic interior or at the aqueous interface. The anchored rhodium complexes efficiently catalyze the reduction of both two-electron substrates (e.g., nicotinamides and flavin) and one-electron substrates (e.g., manganese(III) porphyrins) by sodium formate. Kinetic studies indicate that the rate-limiting step of the reaction is the reduction of the rhodium center by formate, leading to a rhodium(III) hydride or a rhodium(I) species. The three complexes showed different catalytic activities. Cyclic voltammetry and UV–vis measurements revealed that their reduction potentials ($[Rh(III)]^{2+} + 2e^- \rightleftharpoons Rh(I)$) and the p$K_a$ values ($[Rh(III)H]^+ \rightleftharpoons Rh(I) + H^+$) are also different. From the observed trends it is concluded that the catalytic activity of the rhodium complexes depends on its position in the bilayer.

Introduction

Biological membranes play a vital role in many life processes which include transport of ions of normal cell functioning, electron transport, e.g., in the oxidative phosphorylation pathway, charge separation during the complex events of photosynthesis, and the assembling of the components required for the reductive activation of molecular oxygen by the Cytochrome P_{450} enzymes. A number of studies have appeared dealing with artificial systems that mimic certain membrane functions. Some of these studies focus on electron transport across the membrane using mediators like viologens,[1] flavins,[2] and porphyrins[3] which are incorporated in the membrane matrix. In the course of our studies toward the construction of a membrane-bound Cytochrome P_{450} model[4,5] we became interested in developing an efficient catalytic system for the reduction of porphyrins incorporated in the hydrophobic part of a synthetic membrane by a reducing agent present in the aqueous phase.

Studies on the mechanism of the reductive activation of molecular oxygen catalyzed by metalloporphyrins have shown that one of the crucial steps is the fast transfer of two electrons from the reductor via the mediator to the metal center.[6] Further supply of electrons should be prohibited since this leads to the nonproductive degradation of the intermediate active oxygen species (supposedly a high-valent metal–oxo porphyrin[7]) to water. The use of an NADH analogue as the primary reducing agent in combination with a flavin as the electron carrier and a water soluble manganese porphyrin as the catalytic center has proven to be successful.[8] However, one of the problems of this system is the recycling of the NADH. Until a few years ago only the chemical reductor dithionite or enzymes could be used successfully to regenerate NADH.[9] Recently, Steckhan et al. have shown that the combination of sodium formate and a dichloro(pentamethylcyclopentadienyl)(2,2′-bipyridine)rhodium(III) complex (abbreviated as RhCp*(2,2′-bipy)Cl_2) can be applied to convert NAD^+ to NADH.[10] This prompted us to investigate whether this combination of reagents could replace the primary reductor (Pt/H_2) in our previously reported membrane-bound Cytochrome P_{450} mimic and could improve the activity of this model system.

As part of this investigation we report here on the incorporation characteristics and catalytic activity of amphiphilic and polymerizable derivatives of RhCp*-bipyCl_2 in polymerized bilayers of the surfactant *N*-hexadecyl-*N*-(11-(methacryloxy)undecyl)-*N*,*N*-dimethylammonium chloride[11] (MHACl) (Chart 1). Compounds RhC_6 and RhC_{11} differ in the length of the spacer between the methacrylate group and the rhodium complex. We presumed that after copolymerization of the compounds with MHACl the rhodium complex would be positioned at different locations in the bilayer. In the case of RhN the rhodium complex is connected via a spacer to the quarternary ammonium head group. When incorporated in the bilayers of MHACl this rhodium complex has the possibility to shuttle between the aqueous phase and the hydrophobic membrane. We studied the catalytic activity of our rhodium complexes in the reduction of various

® Abstract published in *Advance ACS Abstracts,* February 1, 1995.

(1) Lee, L. Y. C.; Hurst, J. K.; Politi, M.; Kurihara, K.; Fendler, J. H. *J. Am. Chem. Soc.* **1993**, *105*, 370–373.

(2) (a) Tabushi, I.; Hamachi, I.; Kobuke, Y. *J. Chem. Soc., Perkin. Trans. 1* **1989**, 383–390. (b) Kobuke, Y.; Hamachi, I. *J. Chem. Soc., Chem. Commun.* **1989**, 1300–1302.

(3) (a) Nango, M.; Mizusawa, A.; Miyake, T.; Yoshinaga, J. *J. Am. Chem. Soc.* **1990**, *112*, 1640–1642. (b) Nango, M.; Kryu, H.; Loach, P. A. *J. Chem. Soc., Chem. Commun.* **1988**, 697–698. (c) Sakata, Y.; Tatemitsu, H.; Bienvenu, E.; Seta, P. *Chem. Lett.* **1988**, 1625–1628.

(4) van Esch, J. H.; Roks, M. F. M.; Nolte, R. J. M. *J. Am. Chem. Soc.* **1986**, *108*, 6093.

(5) van Esch, J. H.; Feiters, M. C.; Peters, A. M.; Nolte, R. J. M. *J. Phys. Chem.* **1994**, *98*, 5541–5551.

(6) Tabushi, I. *Coord. Chem. Rev.* **1988**, *86*, 1–42.

(7) Ostovic, D.; Bruice, T. C. *Acc. Chem. Rev.* **1992**, *25*, 314–320.

(8) Tabushi, I.; Kodera, M. *J. Am. Chem. Soc.* **1989**, *111*, 1101–1103.

(9) Chenault, H. K.; Whitesides, G. M. *Appl. Biochem. Biotech.* **1987**, *14*, 147–197.

(10) Ruppert, R.; Herrmann, S.; Steckhan, E. *J. Chem. Soc., Chem. Commun.* **1988**, 1150–1151.

(11) Regen, S. L.; Czech, B.; Singh, A. J. *J. Am. Chem. Soc.* **1980**, *102*, 6640.

0022-3263/95/1960-1599$09.00/0

Chart 1

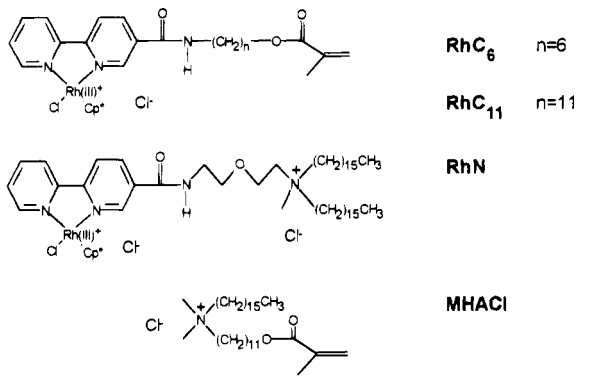

Chart 2

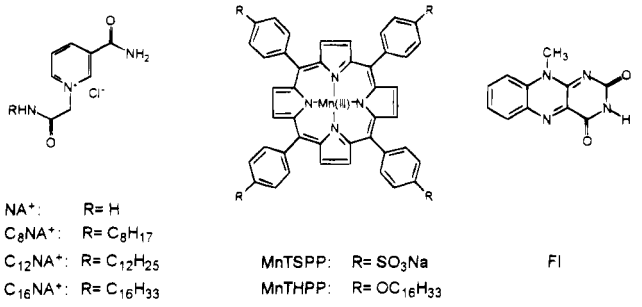

Scheme 1

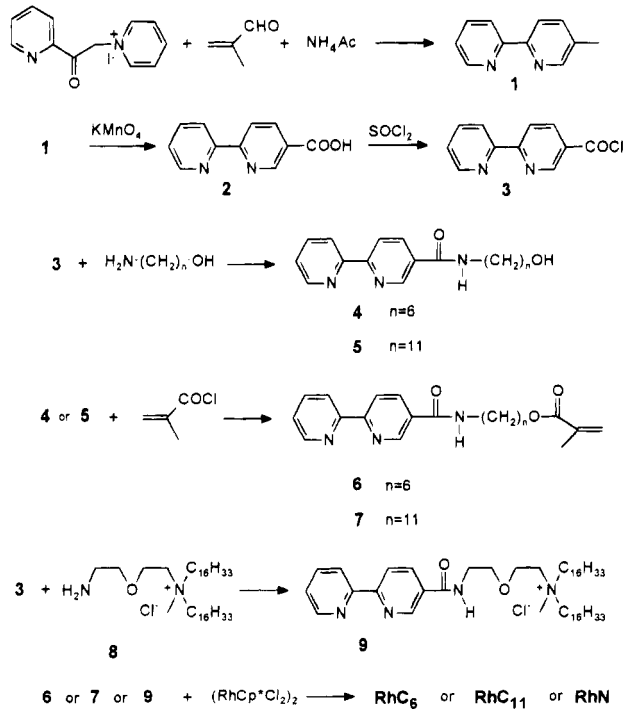

hydrophilic and hydrophobic substrates (Chart 2) by sodium formate. The results are reported here.

Results

Synthesis. The rhodium complexes RhC_6, RhC_{11}, and RhN were synthesized according to Scheme 1. The starting compound 5-methyl-2,2′-bipyridine (**1**) was obtained by condensation of (((2-pyridyl)carbonyl)methyl)-pyridinium iodide, methacrolein, and ammonium acetate in formamide[12] (yellow oil, yield 93%). Compound **1** was oxidized to the carboxylic acid **2** by potassium permanganate in water[13] (yield 50%) and treated with thionyl chloride to give the chlorocarboxy derivative **3**. This unstable yellow solid compound was immediately coupled to 6-aminohexanol or 11-aminoundecanol to give the 2,2′-bipyridine derivatives **4** and **5** as white solids in approximately 51% yield. Reaction of **4** and **5** with methacryloyl chloride and pyridine gave the esters **6** and **7** as white solids in 64% and 59% yield, respectively. The 2,2′-bipyridine surfactant **9** was obtained by coupling of the amine surfactant **8** with **3** (yield 56%).

The 2,2′-bipyridine derivatives **6**, **7**, and **9** were treated with $[RhCp^*Cl_2]_2$ in methanol to give the rhodium complexes RhC_6, RhC_{11}, and RhN, respectively, in high yields.[14] The complexes precipitated from the reaction mixture as yellow solids upon addition of diethyl ether. They readily dissolved in organic solvents such as methanol, ethanol, chloroform, and tetrahydrofuran. Compounds RhC_6 and RhC_{11} also formed optically clear solutions in water. Dissolving RhN in water required heating to 50 °C and vortexing, whereupon an opalescent dispersion was formed. This suggests that this compound forms aggregates, probably bilayer structures (not investigated).

Incorporation. Upon ultrasonic dispersion in water the polymerizable surfactant MHACl forms closed vesicles with a spherical shape, as was confirmed by electron microscopy. The methacrylate moiety in the bilayer of the vesicles can be polymerized by ultraviolet irradiation or by the addition of radical initiators.[11,15] The latter method is known to give the best results; i.e., the polymer chains in the bilayers have the highest molecular weight.[16,17] We therefore chose this procedure (see Experimental Section). UV–vis (disappearance of the band at 205 nm) and ^{1}H-NMR (disappearance of the vinyl proton signals) revealed that polymerization was complete within 2 h.

Incorporation of RhC_6 or RhC_{11} in bilayers of MHACl was investigated by gel permeation chromatography (GPC). GPC of unpolymerized dispersions of MHACl and RhC_6 or RhC_{11} gave two distinct fractions (Figure 1A). The first fraction, eluting with the void volume of the column, contained only MHACl and the second fraction only RhC_6 or RhC_{11}, as was clear from the UV–vis spectra. Apparently, the rhodium complexes had not been incorporated in the unpolymerized bilayers of MHACl. After polymerization the elution profile of the dispersions had changed (Figure 1B). Both fractions still eluted at the same volumes, but the first fraction now contained polymerized MHACl as well as RhC_{11} or RhC_6. The peak area of the second fraction had decreased to approximately 5% of its original value. Apparently, RhC_{11} and RhC_6 were copolymerized with MHACl.

The fraction of initially added RhC_{11} or RhC_6 that was incorporated into the MHACl bilayers by copolymerization ranged from 80 to 90% for a large number of preparations (Table 1). We found that this fraction was independent of the initial molar ratio (f) of RhC_{11} to

(12) Kröhnke, F. *Synthesis* **1976**, 1.
(13) Case, F. H. *J. Am. Chem. Soc.* **1946**, *68*, 2574.
(14) Kölle, U.; Grätzel, M. *Angew. Chem.* **1987**, *99*, 572.
(15) Dorn, K.; Klingbeil, R. T.; Specht, D. P.; Tyminsky, P. N.; Ringsdorf, H.; O'Brien, D. F. *J. Am. Chem. Soc.* **1984**, *106*, 1627–1633.
(16) Bolikal, D.; Regen, S. L. *Macromolecules* **1984**, *17*, 1287–1289.
(17) Dorn, K.; Patton, E. V.; Klingbeil, R. T.; O'Brien, D. F.; Ringsdorf, H. *Makromol. Chem. Rapid Commun.* **1983**, *4*, 513–517.

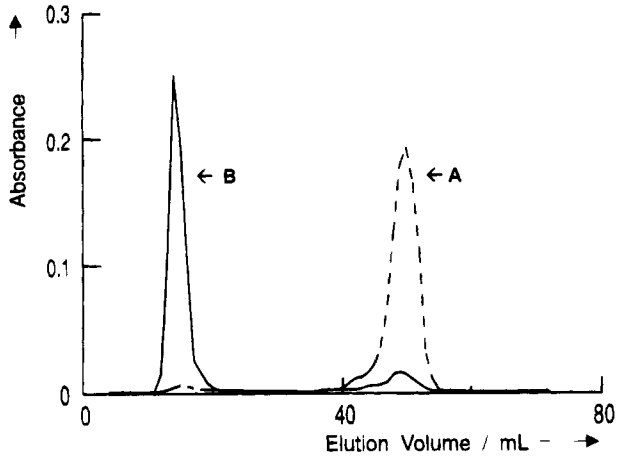

Figure 1. Gel permeation chromatograms of RhC_{11} and MHACl before polymerization (- - -, A) and after polymerization (—, B).

Table 1. Incorporation of Rh Complexes into MHACl Bilayers[a]

complex	f_{Rh}[b]	F_{Rh}[c]	% inc[d]	name[e]
RhC_6	0.1	0.081 ± 0.005	81 ± 5	cop-10-RhC_6
RhC_{11}	0.01	0.0087 ± 0.0025	87 ± 25	cop-1-RhC_{11}
	0.02	0.017 ± 0.002	85 ± 10	cop-2-RhC_{11}
	0.04	0.034 ± 0.002	84 ± 5	cop-4-RhC_{11}
	0.1	0.085 ± 0.004	85 ± 4	cop-10-RhC_{11}

[a] Polymerization was carried out as described in the Experimental Section. [b] Molar ratio of the rhodium complex in the starting mixture: f_{Rh} = [Rh complex]/[MHACl]. [c] Molar ratio of the rhodium complex in the polymerized bilayers. F_{Rh} = [Rh complex]/[MHACl]. The concentration of the rhodium complex in the sample was determined by UV–vis spectroscopy. [d] Percent inc = $(f_{Rh}/F_{Rh})100\%$. [e] The number in the name is $100f_{Rh}$.

MHACl for the range studied (f = 0.01–0.10). The incorporation efficiency was found to be very sensitive to the presence of oxygen during polymerization. Solutions that were not carefully degassed before polymerization showed much lower incorporation efficiencies.

Complete mixing of the rhodium surfactant RhN with the polymerizable surfactant MHACl was achieved by first preparing a mixed film of the two surfactants. To this end a dichloromethane solution that contained both compounds in the appropriate amounts was evaporated. The resulting mixed film was dispersed in water by ultrasonic irradiation, and the obtained bilayers were polymerized as described above. GPC of both the unpolymerized and polymerized dispersions gave very similar elution patterns as the dispersions of cop-10-RhC_6 or cop-10-RhC_6 (for abbreviations see Table 1). This indicates that RhN, in contrast to the latter rhodium complexes, can easily be incorporated in both unpolymerized and polymerized bilayers of MHACl.

Previously, we have shown that incorporation of the metal-free, zinc, or copper derivatives of 5,10,15,20-tetrakis((4-hexadecyloxy)phenyl)porphyrin (THPP) into bilayers of DODAC can lead to aggregation of the porphyrin.[5,18] Incorporation of MnTHPP into bilayers of MHACl could be achieved by injecting an ethanol/THF solution of the porphyrin and the surfactant into water or by sonicating a mixed film of the porphyrin and the surfactant in water. UV–vis spectra showed that the B-band of MnTHPP in dispersions of MHACl prepared by the former method had not shifted compared to the B-band in dichloromethane solutions (λ_{max} = 479 nm) if the surfactant to porphyrin molar ratio was higher than 500/1. Decreasing this molar ratio caused a gradual shift of the B-band maximum to 484 nm at a molar ratio of 100/1. In vesicular solutions prepared by the sonication method the B-band maximum had shifted to 485 nm. The shift of the B-band points to aggregation of the porphyrin.[5] Apparently, MnTHPP does not aggregate in bilayers of MHACl up to high concentrations of porphyrin provided the bilayers are prepared by the ethanol injection method. Anchoring of the rhodium complexes to these MnTHPP-containing bilayers could be achieved by copolymerizing the bilayers with RhC_{11} or by addition of RhN to the ethanolic solutions before injection into water. The other substrates of Chart 2 are water soluble and were added as aqueous solutions (see Experimental Section).

(18) DODAC is *N,N*-dioctadecyl-*N,N*-dimethylammonium chloride.

Table 2. Cyclic Voltammogram Data of Rhodium Complexes[a]

complex	conditions	E_{cat}/ mV	E_{an}/ mV	$E_{1/2}$/ mV	i_{an}/i_{cat}
RhC_6	CH_2Cl_2[b]	−845	−620	−732	~1
RhC_{11}	CH_2Cl_2[b]	−840	−620	−730	~1
RhC_{11}	H_2O, pH 6.9[c]	−660	−535	−598	2.5
RhN	CH_2Cl_2[b]	−845	−625	−735	0.9
cop-10-RhC_6	bilayers, H_2O, pH 6.9[c]	−695	−585	−640	0.6
cop-10-RhC_{11}	bilayers, H_2O, pH 6.9[c]	−645	−575	−610	0.5
cop-10-RhC_{11}	bilayers, H_2O, pH 4.2[c]	−650			<0.1
cop-10-RhN	bilayers, H_2O, pH 6.9[c]	−600	−575	−587	1.3

[a] The potentials are given relative to SSCE. The estimated error is 5%. T = 20 °C. [b] A 1 mM solution of the rhodium complex in CH_2Cl_2 was used, which contained 0.1 M *N,N,N,N*-tetrabutylammonium hexafluorophosphate as the electrolyte. [c] An aqueous buffer of 0.05 M *N*-ethylmorpholine/HCl and 0.05 M NaCl was used.

Electrochemistry. Cyclic voltammograms (CV) of RhC_6, RhC_{11}, and RhN in dichloromethane showed clear reduction and oxidation waves. The i_{an}/i_{cat} values of all three complexes are approximately 1, indicating that the redox reaction is chemically reversible (Table 2). The redox potentials of the complexes in dichloromethane are also given in Table 2. Since the redox-active part of the three rhodium complexes has the same structure it is not surprising that these potentials are nearly the same. Similar results have been reported before for the reduction of Rh(III) to Rh(I) in RhCp*(2,2′-bipy)Cl_2 and derivatives thereof.[14] The large separation between the reduction and oxidation peak is most likely due to two not completely resolved one-electron waves.[19] The redox potential of RhC_{11} was also measured in an aqueous solution of pH 6.9. The $E_{1/2}$ value was found to be 132 mV more positive than in dichloromethane.

Cyclic voltammograms of our rhodium complexes incorporated in polymerized bilayers of MHACl showed clear reduction and oxidation waves (Figure 2). At neutral pH the reduction was reversible. The deviations of the i_{an}/i_{cat} ratio from 1 (Table 2) are due to adsorption of the redox-active species on the electrode, making the reduction and oxidation waves nonsymmetric. The peak currents varied linearly with the scan rate (v) up to 100 mV·s^{-1} (Figure 3). Such a behavior is characteristic for thin films that are adsorbed on electrodes, displaying no electron exchange with nonadsorbed species.[20] When the

(19) Steckhan, E.; Herrmann, S.; Ruppert, R.; Dietz, E.; Frede, M.; Spika, E. *Organometallics* **1991**, 1568–1577.
(20) Murray, R. W. *Electroanalytical Chemistry*; Bard, A. J., Ed.; **1984**, Marcel Dekker: New York, 1984; Vol. 13, pp 191–369.

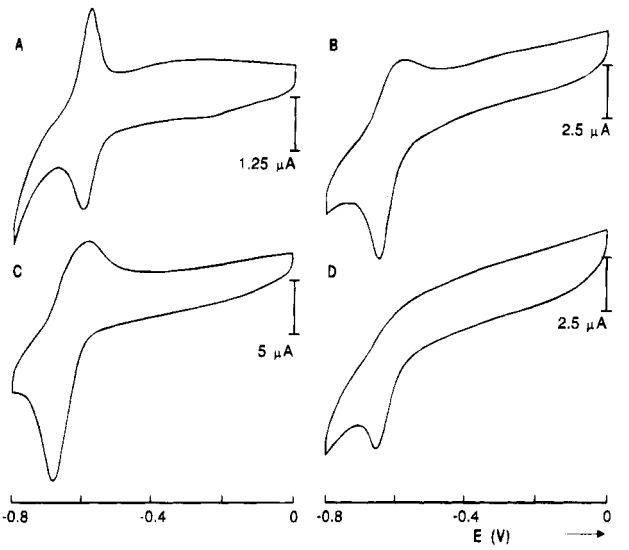

Figure 2. Cyclic voltammograms of aqueous dispersions of cop-10-RhN(A), cop-10-RhC_{11} (B), and cop-10-RhC_6 (C) at pH = 6.9 and of cop-10-RhC_{11} at pH = 4.3 (D).

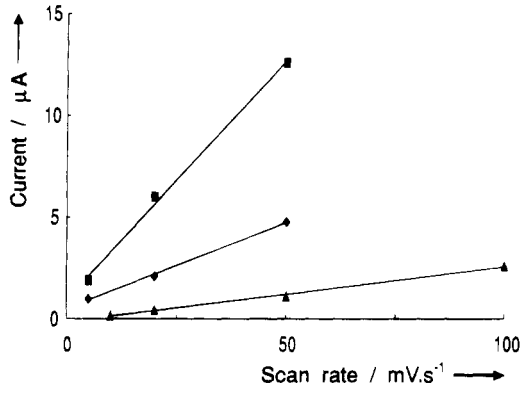

Figure 3. Cathodic peak currents as a function of the scan rate for cop-10-RhN (▲), cop-10-RhC_{11} (◆), and cop-10-RhC_6 (■).

vesicle solution in the electrochemical cell was changed for a buffer solution the reduction and oxidation waves were still observed. Apparently, the polymerized bilayers became strongly adsorbed on the electrode during the measurements. Spontaneous adsorption has been reported before in the literature, *viz.* for dioctadecyldimethylammonium acetate vesicles onto mica substrates.[21] It has been shown that the typical bilayer structure and characteristics are retained during this adsorption process.[22,23]

The total charge Q calculated from the reduction and oxidation waves in the CV can be used to estimate the surface concentration (Γ_0) of the rhodium complexes adsorbed to the electrode, using eq 1 (A is the surface of the electrode).[20]

$$Q = nFA\Gamma_0 \qquad (1)$$

Q was found to be 22×10^{-6} C, 8.3×10^{-6} C, and 2.3×10^{-6} C for cop-10-RhC_6, cop-10-RhC_{11}, and cop-10-RhN, respectively. Accurate determination of Q was troubled by the fact that large charging currents occurred. We estimate the error in Q to be approximately 30%. The Q values correspond to electrode areas per rhodium complex molecule ($1/\Gamma_0$) of 29, 76, and 280 Å^2 for the three catalysts, respectively ($A = 0.78$ cm^2). The concentration of the rhodium complex in the polymerized bilayers was approximately 10 mol %. On the basis of this percentage one would expect to find an electrode-area per rhodium complex of 600 Å^2 when a single is bilayer is adsorbed on the electrode.[24,25] Apparently, in our experiments we are dealing with several bilayers adsorbed on the electrode surface. The polymerized ammonium surfactant is present in a large excess over the rhodium complexes. We may therefore assume that the layer thickness on the electrode is independent of the type of rhodium complex present. The different surface areas found for the three complexes might therefore reflect the different abilities of the rhodium complexes to transport electrons across the bilayers. As the rhodium complexes are covalently anchored to these bilayers, reduction of rhodium in the outer layers most likely occurs via electron hopping from reduced to nonreduced molecules.

Table 2 shows that upon incorporation into bilayers the reduction potentials of the three rhodium complexes become different. Compared to the reduction potential of RhC_{11} in aqueous solutions at pH 6.9 the potentials of cop-10-RhC_6 and cop-10-RhC_{11} have shifted to more negative values whereas that of cop-10-RhN has shifted to a more positive value (Table 2). Apparently, the position of the Rh(III)/Rh(I) equilibrium depends on the location of the rhodium complex in the bilayer.[26]

For cop-10-RhC_{11} at pH 4.2 only one reduction wave was observed (Figure 2). We ascribe this behavior to protonation of the Rh(I) species that is formed after reduction: $Rh(I) + H^+ \rightleftarrows Rh(III)H^+$. The latter species cannot be reversibly oxidized and reduced anymore.[33]

Kinetics. Before carrying out the catalytic reduction experiments it was verified that in the absence of formate or catalyst the substrates were not reduced. Initial experiments revealed that the presence of dioxygen at atmospheric pressure decreased the rate of reduction of the nicotinamides approximately 3-fold and completely inhibited the reduction of Fl and MnTSPP. The reduced forms of the latter substrates are known to be oxidized very fast by molecular oxygen,[27,28] whereas reduced nicotinamides and derivatives are stable in the presence of oxygen.[29] All subsequent measurements were therefore carried out with carefully degassed solutions. The results are presented in Table 3.

Reduction of Nicotinamides. The reduction of $C_{12}NA^+$ and $C_{16}NA^+$ by formate in an aqueous *N*-ethylmorpholine/formic acid buffer at pH 6.9 was efficiently catalyzed by cop-10-RhC_{11} (Table 3, entries 3 and 4). We observed for these substrates a short induction period (~ first 2% of conversion). After this induction period the reaction rate was independent of the substrate concentration up to approximately 70% and 50% conversion for $C_{12}NA^+$ and $C_{16}NA^+$, respectively. At higher conversions precipitation of the product occurred, which obscured further

(21) Pashley, R. M.; McGuiggan, P. M.; Ninham, B. W.; Brady, J.; Evans, D. F. *J. Phys. Chem.* **1986**, *90*, 1637–1642.
(22) Rusling, J. F.; Zhang, H. *Langmuir* **1991**, *7*, 1791–1796.
(23) Rojas, M. T.; Han, M.; Kaifer, A. E. *Langmuir* **1992**, *8*, 1627–1632.
(24) The area per surfactant molecule for the closely related DODAC amounts to approximately 60 Å^2/molecule (ref 25).
(25) Marra, J. *J. Phys. Chem.* **1986**, *90*, 2145–2150.
(26) Rusling, J. F.; Shi, C.-N.; Gosser, D. K.; Shukla, S. S. *J. Electroanal. Chem.* **1988**, *240*, 201–216.
(27) Muller, F. *Top. Curr. Chem.* **1983**, *108*, 71–108.
(28) Tsuchida, E.; Nishide, H. *Top. Curr. Chem.* **1986**, *132*, 63–100.
(29) Norris, D. J.; Stewart, R. *Can. J. Chem.* **1977**, *55*, 1687–1695.

Table 3. Turnover Numbers for the Reduction of Substrates by Membrane-Bound Rhodium Complexes[a]

entry	substrate	catalyst	counterion[b]	[formate][c]	10^3 TO[d]/s^{-1}
1	NA^+	cop-10-RhC_{11}	bromide	0.294	~0.1
2	C_8NA^+[e]				1.8
3	$C_{12}NA^+$[e]				3.1
4	$C_{16}NA^+$[e]				3.2
5	Fl[f]			0.147	3.1
6	Fl[g]	cop-10-RhC_{11}	chloride		10.9
7	MnTSPP[h]				16.7
8	MnTSPP[i]	cop-1-RhC_{11}			15.3
9	Fl[k]	cop-10-RhC_6			3.1
10	Fl[l]	cop-10-RhN			15.8

[a] For reaction conditions see the Experimental Section. Since the concentrations of the rhodium complexes vary per preparation of the catalyst the final concentrations of the rhodium complex in the reaction mixtures are given in footnotes e–l. [MHACl] = 5×10^{-4} M; T = 37.5 °C. [b] The catalyst containing bromide ions was prepared from cop-10-RhC_{11} by ion exchange chromatography (see Experimental Section). [c] Total formate concentration, including formate of the buffer. [d] TO is turnover frequency (mol product per mol rhodium complex per s). The estimated error is 5%. [e] [Substrate] = 2.5×10^{-4} M; [RhC_{11}] = 5.5×10^{-5} M. [f] [Substrate] = 6.1×10^{-5} M; [RhC_{11}] = 5.5×10^{-5} M. [g] [Substrate] = 6.1×10^{-5} M; [RhC_{11}] = 4.1×10^{-5} M. [h] [Substrate] = 3.75×10^{-5} M; [RhC_{11}] = 4.1×10^{-5} M. [i] [Substrate] = 3.75×10^{-5} M; [RhC_{11}] = 3.5×10^{-6} M. [k] [Substrate] = 6.1×10^{-5} M; [RhC_6] = 6.75×10^{-5} M. [l] [Substrate] = 6.1×10^{-5} M; [RhN] = 4.3×10^{-5} M.

observations. The turnover numbers were approximately the same for both substrates. C_8NA^+ can also be reduced by cop-10-RhC_{11}, but the rate of reduction is approximately half the rate observed for $C_{12}NA^+$ and $C_{16}NA^+$ (Table 3, entry 2). NA^+,[30] which has no additional hydrophobic substituent, was only converted very slowly (Table 3, entry 1). These results suggest that the reduction reaction takes place on the surface of the bilayers. The presence of a large hydrophobic substituent on the positively charged nicotinamides is necessary for binding as it compensates for the electrostatic repulsion that exists between the substrate and the bilayer surface. We did not further investigate the kinetics of the reduction of these nicotinamides.

Reduction of Fl. The flavin Fl, which does not bear a charge, was effectively reduced by cop-10-RhC_{11} (Table 3, entry 5). An induction period was not observed, and the reaction was zero order in substrate up to 90% conversion. When chloride was the counterion instead of bromide the rate of reduction increased approximately 3-fold (Table 3, entry 6). Furthermore, the rate of reduction of the flavin was found to be independent of the pH in the range 4.4–7.

We found for the reduction of Fl by a series of cop-n-RhC_{11} catalysts (n = 1–10) a linear relation between the reaction rate and the concentration of RhC_{11} at a constant surfactant concentration (Figure 4). The turnover numbers of these catalysts amounted to 0.013 s^{-1} (Figure 4 inset). Table 3 shows that on incorporation into polymerized bilayers of MHACl the catalytic activities of the three rhodium complexes become different. We found that cop-10-RhC_6 was a less efficient catalyst than cop-10-RhC_{11} whereas cop-10-RhN was a more efficient catalyst for the reduction of Fl (Table 3, entries 6, 9, and 10). For cop-10-RhC_6 and cop-10-RhN the reduction of Fl was also independent of the substrate concentration, suggesting that reduction of the rhodium complex by formate is the rate determining step.

(30) Stewart, R., Norris, D. J. *J. Chem. Soc., Perkin Trans. 2* **1978**, 246–249.

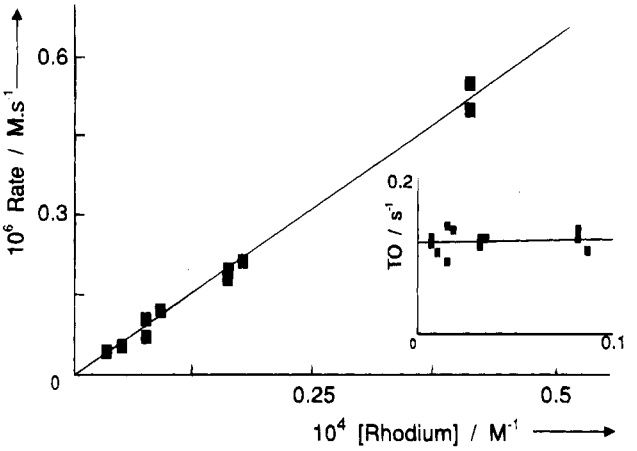

Figure 4. Catalytic activity of bilayer-anchored RhC_{11} in the reduction of Fl as a function of the rhodium concentration at constant MHACl concentration. Inset: Turnover numbers for the reduction of Fl by the same series of catalysts as a function of the RhC_{11} to MHACl molar ratio. [MHACl] = 5×10^{-4} M, T = 37.5 °C.

The activation energies for the reduction of Fl by cop-10-RhC_{11} and cop-1-RhC_{11} were calculated from the slopes of the Arrhenius plots and were found to be 109 ± 8 and 104 ± 3 kJ/mol, respectively. These values are somewhat larger than the activation energy of 88 kJ/mol reported for the reduction of NAD^+ catalyzed by RhCp*-(2,2′-bipy)Cl_2.[10] The activation energy for cop-10-RhC_6 amounted to 117 ± 6 kJ/mol which is an even larger value than found for cop-10-RhC_{11}.

Reduction of Manganese Porphyrins. Both the nicotinamides and the flavin are two-electron substrates which are very likely to be reduced by a rhodium hydride species in a reaction that has a one to one stoichiometry (*vide infra*). The rhodium-catalyzed reduction reaction appeared not to be limited to these two-electron substrates. The one-electron substrate Mn(III)TSPP was also very efficiently reduced, *viz.* to a manganese(II) porphyrin, again in a zero-order reaction. We found for the reduction of MnTSPP almost identical turnover numbers when cop-10-RhC_{11} or cop-1-RhC_{11} were used as the catalysts (Table 3, entries 7 and 8). The activation energies were also rather similar, *viz.* 86 ± 4 and 92 ± 6 kJ/mol, respectively. Apparently, the catalytic activity of RhC_{11} in the reduction of MnTSPP is independent of the surfactant to RhC_{11} ratio within the range studied.

Addition of a formate solution to polymerized MHACl solutions containing 0.2 mol % Mn(III)THPP and varying concentrations of RhN or RhC_{11} led to a fast one-electron reduction of the porphyrin. In the presence of approximately 1 mol % of RhN or RhC_{11} the formation of Mn(II)THPP showed first-order kinetics. The pseudo-first-order rate constants amounted to 0.016 and 0.0022 s^{-1}, respectively. We found that in the case of RhN the initial rates were independent of the rhodium concentration in the investigated range of 0.3–1.0 mol % of RhN in MHACl. For RhC_{11} the rates increased with increasing concentration of the rhodium complex in the same concentration range.

Formate Concentration Dependence. The dependence of the rate of reduction of Fl on the formate concentration is shown in Figure 5. At low concentrations the rate is proportional to the formate concentration. At higher concentrations ([$HCOO^-$] > 0.1 M) the rates level off. These observations are in line with the mechanism

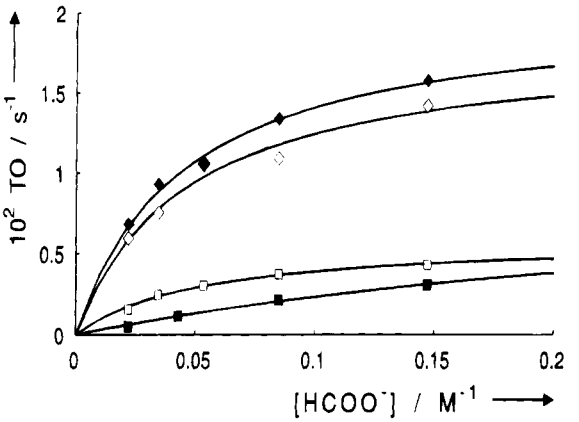

Figure 5. Turnover frequencies for the reduction of Fl as a function of the formate concentration for cop-10-RhN (◆), cop-10RhC$_{11}$ (◇), and cop-10-RhC$_6$ (□), with chloride as the counterion of the polymerized bilayers and for cop-10-RhC$_{11}$ with bromide as the counterion (■); T = 37.5 °C.

Table 4. Experimentally Determined Values of the Constants in Eq 4 and Experimentally Determined pK_a^{obs} for the Various Catalysts[a]

catalyst	counterion	$(K')^{-1}/M^{-1}$	$10^2\,k/s^{-1}$	pK_a^{obs}
RhC$_6$				7.6
cop-10-RhC$_6$[b]	chloride	19.1	0.59	6.7
cop-10-RhC$_{11}$[c]	bromide	2.9	1.03	
cop-10-RhC$_{11}$[d]	chloride	21.7	1.82	5.3
cop-10-RhC$_{11}$[e]	chloride	22.2	2.05	4.3

[a] K' and k are defined by eq 4. The measurements were carried out as described in the Experimental Section. Since the concentrations of the rhodium complexes vary per preparation of the catalyst their concentrations in the reaction mixtures are given in footnotes b–d. [MHACl] = 5 × 10^{-4} M; T = 37.5 °C. [b] [RhC$_6$] = 6.75 × 10^{-5} M. [c] [RhC$_{11}$] = 5.0 × 10^{-5} M. [d] [RhC$_{11}$] = 4.75 × 10^{-5} M. [e] [RhN] = 4.3 × 10^{-5} M.

proposed by Steckhan et al.[10] for the reduction of NAD$^+$ by formate catalyzed by RhCp*(2,2′-bipy)Cl$_2$. According to these authors the rate-determining step of the reduction reaction is the decomposition of a Rh(III) formate complex that is formed in a equilibrium preceding the rate-determining step: Rh(III)$^{2+}$ + HCOO$^-$ ⇄ [Rh(III)-HCOO]$^+$ → product. In our case the situation is complicated by the fact that the concentrations of the reactants in the proximity of the bilayer surface will differ from the concentrations in bulk solution. It is, however, reasonable to assume that no specific adsorption of formate on the positively charged bilayer will take place.[31,34] In that case it is sufficient to consider only the coordination of formate anions to the rhodium complex. If excess formate is present, the concentration of the rhodium formate complex is related to the total concentration of rhodium complex ([Rh(III)$_{tot}^{2+}$]) by eq 2. In this

$$[\mathrm{Rh(III)(HCOO)^+}] = \frac{K_b[\mathrm{HCOO^-}]_x[\mathrm{Rh(III)}^{2+}_{tot}]}{1 + K_b[\mathrm{HCOO^-}]_x} \quad (2)$$

$$[\mathrm{HCOO^-}]_x = [\mathrm{HCOO^-}]_\infty\, e^{\left(\frac{F\psi(x)}{RT}\right)} \quad (3)$$

equation [HCOO$^-$]$_x$ is the concentration of the formate anion at the site on the bilayer interface where the rhodium complex is located and K_b is the binding

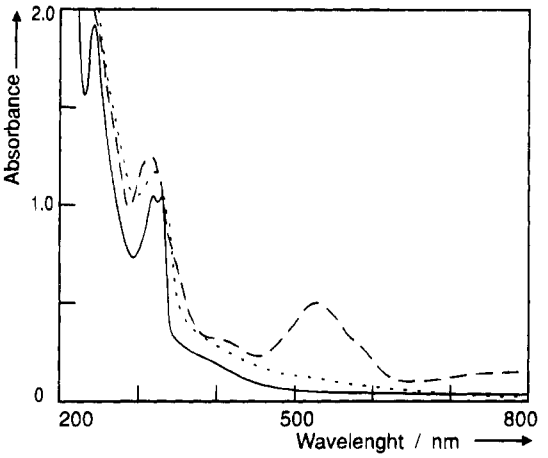

Figure 6. UV–vis absorption spectra of cop-10-RhC$_{11}$ in water (—), of cop-10-RhC$_{11}$ in formate buffer at pH 6.9 (– – –), and of cop-10-RhC$_{11}$ in formate buffer at pH 4.4 (– – –). [RhC$_{11}$] = 5.9 × 10^{-5} M; [HCOO$^-$] = 0.147 M; T = 37.5 °C.

constant for coordination of formate to the rhodium complex. The Boltzmann equation (3) relates [HCOO$^-$]$_x$ to the bulk concentration of formate ([HCOO$^-$]$_\infty$).[32] In this equation $\psi(x)$ is the surface potential of the bilayer at the site of the rhodium complex. Combination of eqs 2 and 3 eliminates [HCOO$^-$]$_x$. We assume that the rate of reduction is proportional to the concentration of Rh-(III)(HCOO)$^+$ with rate constant k. The relation between the formate concentration in the aqueous bulk phase and the rate of reduction is then given by eq 4, in which the latter rate is expressed as the turnover frequency (TO).

$$\mathrm{TO} = \frac{k[\mathrm{HCOO^-}]_\infty}{K' + [\mathrm{HCOO^-}]_\infty} \quad \text{with } K' = K_b^{-1}\, e^{\left(-\frac{F\psi(x)}{RT}\right)} \quad (4)$$

The experimental curves in Figure 5 can be fitted very well to this equation. The resulting values for k and $(K')^{-1}$ are given in Table 4. As can be seen from this table, the values of $(K')^{-1}$ for the various rhodium complexes are not significantly different. As the surface potentials probably will not differ very much, the K_b values will also have similar values. The main cause for the differences in the catalytic activity of the three catalysts lies in the differences in the rate constants k.

When bromide ions are present as the counterions of the polymerized bilayers, the rate of reduction is decreased by a factor of ~3 (Table 3, entries 5 and 6). Table 4 reveals that this is the result of a 7-fold reduction of the apparent association constant $(K')^{-1}$. The rate constant k is also decreased, but only by a factor of 1.6. It is known that the surface potential of quaternary ammonium bilayers is strongly decreased by bromide counterions, even when these ions are present in small quantities.[21]

Formation of Rh(I) Species. In the absence of substrate, addition of formate to aqueous dispersions of cop-10-RhC$_{11}$ (pH 6.9) caused a color change from yellow to violet. The UV–vis absorption spectrum showed the development of a broad band at 520 nm (Figure 6). We ascribe this band to a Rh(I) complex.[33] It has been shown by ^{1}H-NMR spectroscopy that reduction of Rh(III) by

(31) Frausto da Silva, J. J. R.; Williams, R. J. P. *Struct. Bond.* **1976**, *29*, 102–120.

(32) McLaughlin, S. *Curr. Top. Membr. Transport* **1977**, 71–144.

(33) Kolle, U.; Kang, B.-S.; Infelta, P.; Comte, P.; Grätzel, M. *Chem. Ber.* **1989**, *122*, 1869–1880.

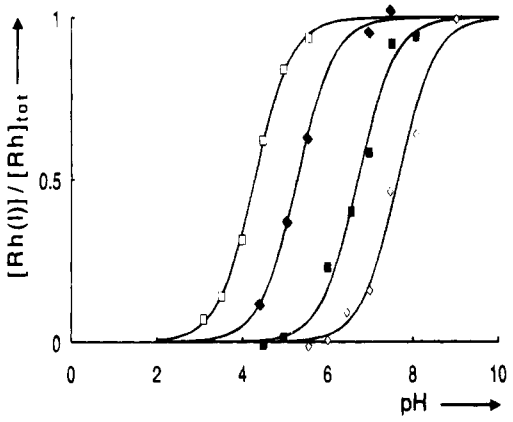

Figure 7. Fraction of Rh(I) obtained after reduction with formate as a function of the pH for cop-10-RhN (□), cop-10-RhC_{11} (◆), cop-10-RhC_6 (■), and RhC_6 (◇). T = 37.5 °C.

formate initially gives a rhodium(III) hydride, most likely via a hydride transfer from the formate anion to the Rh(III) metal center.[19] Apparently, under the conditions of our experiments, this initially formed Rh(III) hydride decomposes into a Rh(I) complex ($Rh(III)H^+ \rightleftarrows Rh(I) + H^+$, *vide infra*). Reduction of Rh(III) at pH = 4.4 did not result in formation of a band at 520 nm (Figure 6). This indicates that at this pH the Rh(III) hydride is stable.

The pK_a of the Rh(III)H complex can be determined by measuring the $[Rh(I)]/[Rh]_{tot}$ ratio as a function of the pH. The results for the various catalysts are presented in Figure 7. The experimental curves can be fitted very well by a single acid–base dissociation equilibrium. The resulting pK_a values (pK_a^{obs}) are given in Table 4. It is clear that incorporation of the rhodium complexes in the bilayers has a large effect on pK_a^{obs}. Compared to the pK_a value found for RhC_6 in aqueous solution without surfactant, the pK_a^{obs} values of the membrane-bound rhodium complexes have decreased by 0.9–3.3 pH units. The relatively high acidity of the membrane-bound rhodium species is due to the surface potential of the positively charged bilayer. The pK_a^{obs} is related to the intrinsic or interfacial pK_a^i by eq 5.[34] This intrinsic pK_a^i

$$pK_a^{obs} = pK_a^i - \frac{F\psi(x)}{2.303RT} \qquad (5)$$

is the pK_a in the absence of any surface potential. Its value depends on the relative stabilities of the species involved in the equilibrium at the site of residence of the rhodium complex.[35]

The extinction coefficients of the absorption band at 520 nm of the Rh(I) form of the three catalysts were very similar and amounted to (8600 ± 400) $M^{-1}cm^{-1}$. This value is in good agreement with the extinction coefficient of the Rh(1) species formed by RhC_6 in homogeneous aqueous solution. This indicates that the bilayer-anchored rhodium complexes were completely reduced to the Rh(I) species by formate. Furthermore, we found that for cop-10-RhC_{11} the formation of the band at 520 nm took place in a first-order reaction at 37.5 °C and pH 6.9. The first-order reaction constant amounted to (0.013 ± 0.001) s^{-1} at a formate concentration of 0.147 M.

(34) Fernandez, M. S.; Fromherz, P. *J. Phys. Chem.* **1977**, *81*, 1755–1761.

(35) Drummond, C. J.; Grieser, F.; Healy, T. W. *J. Chem. Soc., Faraday Trans. 1* **1989**, *85*, 521–535.

Discussion

Catalysis in micellar or bilayer systems can be described by a so-called pseudophase model. In this model reactions take place in the polar aqueous phase and in the apolar micellar or membrane phase.[36,37] The GPC experiments reported in the Results suggest that the rhodium complexes RhC_6, Rh_{11}, and RhN are strongly bound to the MHACl membrane pseudophase.[38] We also observed that in the absence of the bilayer-anchored rhodium catalyst no reduction of the substrates occurred. These combined data indicate that for the discussion below we only have to consider reductions occurring in the membrane pseudophase.[38] We found that the rate of reduction of the nicotinamides strongly depends on the hydrophobicity of the substrate: the turnover numbers increase in the series $NA^+ < C_8NA^+ < C_{12}NA^+, C_{16}NA^+$. The very slow reduction of NA^+ is most likely the result of an unfavorable partition of this compound over the aqueous phase and the membrane phase. Increasing the hydrophobicity of the substrate causes the partition equilibrium to shift toward the membrane phase with a faster reduction reaction as a result. In the case of Fl and MnTSPP the rate of reduction was independent of the substrate concentration up to high conversions. This indicates either that the membrane phase is saturated with substrate or that the substrate is strongly bound to the membrane phase. The fact that the reduction rates of Fl and MnTSPP are comparable to or larger than the reduction rates of the most hydrophobic nicotinamides $C_{12}NA^+$ and $C_{16}NA^+$ is in favor of the latter possibility. In the following discussion we will therefore ignore the effects of substrate partitioning between the aqueous and the membrane pseudophase for these two substrates.

Our polymerized catalysts form spherically closed vesicles in water. We did not get any indication that the reactivity of the rhodium complexes anchored to the outer bilayer-half is different from that of the rhodium complexes anchored to the inner bilayer-half. We observed that reduction with formate gave a complete conversion of the Rh(III) complexes to their Rh(I) redox state in a first-order reaction. An explanation for this observation may be that the rhodium complexes are able to transport electrons across the vesicle bilayers. This explanation is supported by the electrochemical measurements and by the fact that MnTHPP, which is located in the hydrophobic part of the bilayer,[5] is also reduced by the vesicle-anchored rhodium complexes. Another reason for the above-mentioned observations could be that the vesicles leak under the conditions of our experiments.

We observed for our rhodium complexes anchored to the polymerized bilayers that the rate of reduction of Fl is first order in rhodium concentration and zero order in

(36) Fendler, J. H.; Hinze, W. L. *J. Am. Chem. Soc.* **1981**, *103*, 5439–5447.

(37) Berezin, I. V.; Martinek, K.; K. Yatsimirskii, K. *Russ. Chem. Rev.* **1973**, *42*, 787–802.

(38) A reviewer suggested two alternative interpretations of the GPC data: (i) RhC_6 and RhC_{11} polymerize either as monomer or as micelles in the presence of MHACl vesicles in the bulk exterior phase and are not associated with the bilayers. When the degree of polymerization is high enough, poly(RhC_6) and poly(RhC_{11}) are eluted in the void volume along with the vesicles. (ii) The vesicles act as a "seed" from which the poly(RhC_6) or poly(RhC_{11}) grow outward into the bulk aqueous phase. In that case, the catalyst would be membrane-linked, but not positioned within the bilayer. Although we cannot exclude that these processes also play a role during polymerization, they do not account for the results obtained from our kinetic and electrochemical studies.

substrate concentration. Furthermore, the rate depended in a Michaelis–Menten type of fashion on the formate concentration (Figure 5). These observations are in line with the mechanism proposed by Steckhan et al. for the RhCp*(2,2'-bipy)Cl_2-catalyzed reduction of NAD^+ by formate.[10] These authors assume a pre-equilibrium in which formate coordinates to the rhodium complex. In a subsequent step, which is probably the rate-determining step, the Rh(III)–formate complex decomposes into a Rh(III)–hydride and carbon dioxide. In the last step a very fast reduction of the substrate takes place. Since the structures of our rhodium complexes are the same, except for the substituent on the bipyridine ligand, the different reactivities found for the bilayer-anchored rhodium catalysts must be explained from the fact that the catalysts are located at different positions with respect to the bilayer surface (Figure 8). These different locations have a clear effect on the electrochemical properties of the complexes. Equations 6 and 7 describe

$$[\mathrm{Rh(II)X}^n]_{aq}^{(2+n)+} \underset{-2e}{\overset{2e}{\rightleftharpoons}} [\mathrm{Rh(I)}]_{aq} + \mathrm{X}^n_{aq} \qquad (\mathrm{X}^n = \mathrm{Cl}^- \text{ or } \mathrm{H_2O}) \quad (6)$$

$$[\mathrm{Rh(III)X}^n]_{int}^{(2+n)+} \underset{-2e}{\overset{2e}{\rightleftharpoons}} [\mathrm{Rh(I)}]_{int} + \mathrm{X}^n_{aq} \quad (7)$$

the electrochemical reduction and oxidation processes of the rhodium complexes in water and at the interface of the polymerized bilayers, respectively. These processes are characterized by the reduction potentials $E_{1/2}{}^{aq}$ and $E_{1/2}{}^{i}$. The differences of these reduction potentials, $\Delta E_{1/2} = E_{1/2}{}^{i} - E_{1/2}{}^{aq}$, reflect the effect of the microenvironment on the equilibria.[26] These $\Delta E_{1/2}$ values can be calculated from the data in Table 2 and are presented in Table 5. The differences in the free energy ΔG (eq 8)

$$\Delta G = [\mu(\mathrm{Rh(I)})_{int} - \mu(\mathrm{Rh(III)X}^n)_{int}^{(2+n)+}] - [\mu(\mathrm{Rh(I)})_{aq} - \mu(\mathrm{Rh(III)X}^n)_{aq}^{(2+n)+}] \quad (8)$$

can be derived from $\Delta E_{1/2}$ and are also tabulated in Table 5. As can be seen in Table 5 the reduction of cop-10-RhN occurs more easily than the reduction of RhN in the bulk aqueous phase ($\Delta E_{1/2} > 0$).[39] This can be understood since the former catalyst is located at the aqueous interface of the bilayer. The dielectric constant of the interface is lower than the dielectric constant of the bulk aqueous phase.[34,37] In a medium with a lower dielectric constant equilibrium 7 will shift in the direction of the uncharged Rh(I) complex. Remarkably, in the case of cop-10-RhC_6 and to a lesser extent of cop-10-RhC_{11} reduction of the rhodium center becomes more difficult ($\Delta E_{1/2} < 0$). This indicates that upon incorporation into the polymerized bilayer the Rh(III) species becomes stabilized relative to the Rh(I) species. This could point to a specific medium effect. The hydration spheres of the rhodium centers in cop-10-RhC_6 and cop-10-RhC_{11} may interact differently with the hydration spheres of the quaternary ammonium head groups than the hydration sphere of the rhodium center in cop-10-RhN. It is also possible that the charged rhodium complexes in cop-10-RhC_6 and cop-10-RhC_{11} are not located at the aqueous interface but in the hydrophobic interior of the membrane. Here a specific medium effect could result through

(39) We assume that the value of $E_{1/2}{}^{aq}$ of RhN in the absence of any aggregation is equal to that of RhC_{11}.

Table 5. Various Parameters of Bilayer-Anchored Rhodium Complexes

catalyst	$\Delta E_{1/2}{}^{a}$/V	ΔG/kJ·mol^{-1}	ΔpK	$pK_a{}^{i}$	ψ_x/V
cop-10-RhC_6	−0.042	8.1	1.44	9.1	0.142
cop-10-RhC_{11}	−0.012	2.3	0.41	8.0	0.159
cop-10-RhN	+0.011	−2.1	−0.37	7.3	0.177

[a] $\Delta E_{1/2} = E_{1/2}{}^{i} - E_{1/2}{}^{aq}$. The aqueous reduction potentials of RhC_6 and RhN are assumed to be equal to the reduction potential of RhC_{11}: $E_{1/2}{}^{aq} = -0.598$ V (Table 2).

interaction of the rhodium centers with the ester groups of the polymer backbone.

The rhodium(III) hydride formed after reduction by formate is in equilibrium with a rhodium(I) complex. The corresponding equations for the aqueous phase and the membrane phase are given by eqs 9 and 10, respectively.

$$[\mathrm{Rh(III)H}]^+_{aq} \overset{pK_a{}^{aq}}{\rightleftharpoons} [\mathrm{Rh(I)}]_{aq} + \mathrm{H}^+_{aq} \quad (9)$$

$$[\mathrm{Rh(III)H}]^+_{int} \overset{pK_a{}^{i}}{\rightleftharpoons} [\mathrm{Rh(I)}]_{int} + \mathrm{H}^+_{aq} \quad (10)$$

$$\Delta G_a = [\mu(\mathrm{Rh(I)})_{int} - \mu(\mathrm{Rh(III)H})^+_{int}] - [\mu(\mathrm{Rh(I)})_{aq} - \mu(\mathrm{Rh(III)H})^+_{aq}] \quad (11)$$

For the difference between the intrinsic or interfacial $pK_a{}^{i}$ and the pK_a in aqueous solution we can write $\Delta pK_a = pK_a{}^{i} - pK_a{}^{aq} = -\Delta G_a/2.303RT$ (eqs 9–11). Using ΔG from the electrochemical measurements (at 293 K) as an approximation for ΔG_a (at 310 K) we can calculate the surface pK_a and from this with eq 5 and pK_{obs} from Table 4 the surface potentials ψ_x for our rhodium complexes incorporated into the polymerized bilayers. The result is presented in Table 5. Considering the assumptions made, the calculated surface potentials agree very well with values reported in the literature for dioctadecyldimethylammonium bilayers.[25] The result should nevertheless be interpreted with caution, especially with regard to whether the differences in the surface potentials between the three complexes are significant. Assuming an average surface potential of 0.16 V one can calculate using the Gouy equation[33] that the average surface charge density on our polymerized bilayers is 1 positive charge per 195 Å^2. This value is considerably lower than the value of 1 charge per 60 Å^2, which one would expect to find if the charge on each surfactant molecule is not compensated. Apparently, the positive charge is partly compensated for by binding of anions. It is known that formate anions behave like fluoride or acetate anions.[31] These ions do not bind to the surface of quaternary ammonium bilayers.[25] The charge compensation therefore is most likely the result of binding of chloride ions, despite the fact that these ions are present in low concentrations.

The overall binding constant for formate $(K')^{-1}$ is related to the binding constants K_b via the Boltzmann equation (see eq 4). Using averaged values of 21 M^{-1} (Table 4) and 0.16 V (Table 5) for $(K')^{-1}$ and ψ_x, respectively, we obtain an average binding constant K_b for the three rhodium complexes of 0.053 M^{-1}. This value is much smaller than the value of 7.1 M^{-1}, reported for the binding constant of formate to Rh(III)Cp*(2,2'-bipy)Cl_2.[10] The latter constant was, however, measured at very low chloride ion concentrations (5×10^{-5} M) in aqueous solutions without any other ligand or surfactant present. These conditions will strongly favor coordination of a

water molecule to the rhodium complex. We attribute our lower binding constant to a competition between formate ions and chloride ions. Water molecules will probably play no role. In the presence of bromide ions the overall binding constant is even lower. It is clear that this decrease will be the result of both a further lowering of the surface potential by binding of bromide ions to the bilayers and a stronger binding of the bromide ion to the rhodium complex.

Although the presence of small concentrations of chloride ions has a strong effect on the binding of the formate ions, this feature does not alter the maximum rates of reduction. The maximum turnover number expressed by k in eq 4 is dependent on the rate of decomposition of the rhodium formate complex into a rhodium(III) hydride complex. Apparently, the main cause for the observed different reactivities of the polymer-anchored rhodium complexes is the effect of the microenvironment on the stabilities of the rhodium formate complexes and on the relative energies of the transition states of the reduction reaction. This also follows from the observed different activation energies for the reductions catalyzed by cop-10-RhC_6 and by cop-10-RhC_{11}. Probably similar effects of the microenvironment on the relative stabilities of these species play a role as with the acid–base equilibria and the electrochemical equilibria.

Scheme 2

$$[Rh(III)]^{2+} + HCOO^- \underset{k_{-1}}{\overset{k_1}{\rightleftharpoons}} [Rh(III)HCOO]^+ \quad (12)$$

$$[Rh(III)HCOO]^+ \xrightarrow{k_2} [Rh(III)H]^+ + CO_2 \quad (13)$$

$$[Rh(III)H]^+ \underset{k_{-3}}{\overset{k_3}{\rightleftharpoons}} [Rh(I)] + H^+ \quad (14)$$

$$[Rh(III)H]^+ + Fl \xrightarrow{k_4} [Rh(III)]^{2+} + FlH^- \quad (15)$$

$$[Rh(I)] + Fl \xrightarrow{k_5} [Rh(III)]^{2+} + Fl^{2-} \quad (16)$$

$$I^{2-} + H^+ \rightarrow FlH^- \quad (17)$$

$$IH^- + H^+ \rightarrow FlH_2 \quad (18)$$

Finally, we would like to return to the mechanism of the reduction reaction. The important equations for the reduction of Fl are eqs 12–18 of Scheme 2. The second-order rate constants for protonation of various Rh(I)Cp*-(2,2′-bipy) complexes (k_{-3} in eq 14) have been reported in the literature.[33] They range from 10^7 to 10^9 M^{-1} s^{-1}. The pk_a^i of cop-10-RhC_{11} amounts to 8.0 (Table 4), which corresponds to an equilibrium constant of 10^{-8} M. From these data it can be calculated that k_3 in eq ranges from 0.10 to 10 s^{-1}. The rate constant k in eq 4 is equal to k_2 in eq 13. Since this constant (see Table 4) is smaller than k_3 we may conclude that the formation of the Rh(I) complex becomes an important process above the pK_a of the rhodium(III)–hydride. Which of these species will be dominant in the reduction of Fl will not only depend on the pH but also on the values of the rate constants k_4 and k_5 in eqs 15 and 16, respectively. Since we observed that the rate of reduction of Fl is independent of the pH in the range pH 4.2–7, we may conclude that in this pH range protonation of reduced Fl (eqs 17 and 18) will not be rate limiting.

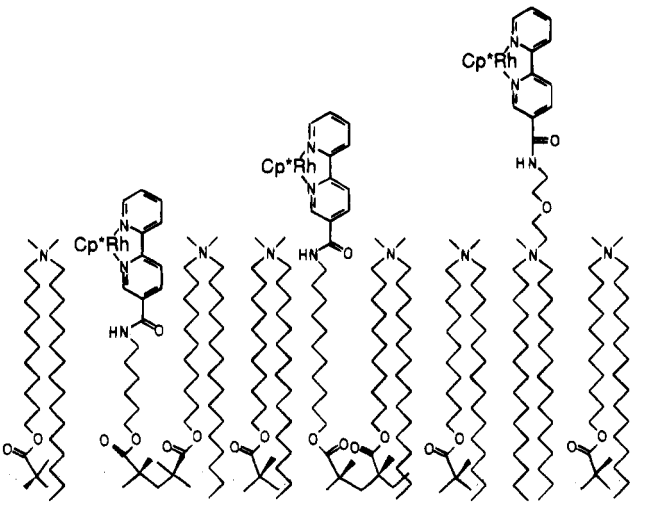

Figure 8. Impression of the arrangement of the rhodium complexes in half of a polymerized bilayer of MHACl vesicles.

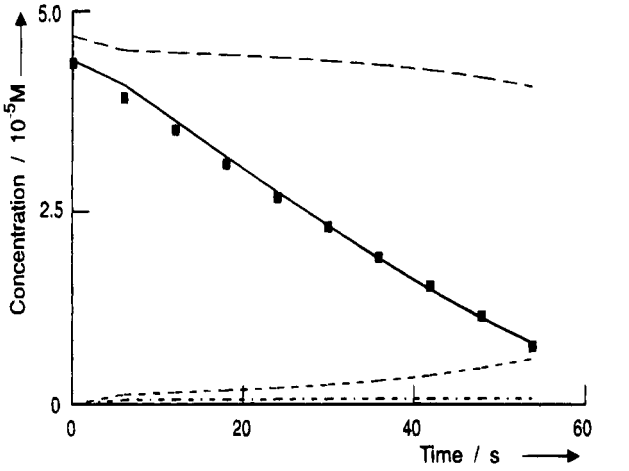

Figure 9. Concentrations of the various species during the reduction of Fl catalyzed by cop-10-RhC_{11}. Experimentally determined concentration of Fl (■) and calculated concentration of Fl (—), Rh(III) (– –), Rh(III)H(· – – –), and Rh(I) (- - – –), according to eqs 13–16 of Scheme 2; $k_2 = 0.0018$ s^{-1}; $k_3 = 1$ s^{-1}; $k_{-3}[H^+] = 0.1$ s^{-1}; $k_4 = k_5 = 10^4$ M^{-1} s^{-1}. Time interval between the calculated concentrations was 0.05 s.

The equations in Scheme 2 can be used to calculate the concentration of each of the reactants as a function of time (Figure 9). These calculations predict that the flavin concentration will decrease linearly with time if the second-order rate constant k_4 or k_5 is equal to or larger than 10^3 M^{-1}·s^{-1}. A good agreement with the experimental rate of reduction of Fl was obtained for k_5-(k_4) = 10^4 M^{-1}·s^{-1}.

The results presented in the Results show that our bilayer anchored rhodium complexes are also efficient catalysts for the reduction of manganese porphyrins. This holds for porphyrin molecules present at the aqueous interface (MnTSPP) and for porphyrin molecules located in the hydrophobic interior of the bilayer (MnTHPP). From the zero-order dependence of the rate on the MnTSPP concentration it can be concluded that the reduction of the manganese porphyrin is much faster than the formation of the rhodium–hydride complex. This result is promising as we want to use the present

system as a mimic of the membrane bound Cytochrome P_{450} monooxygenase.

The reduction of Mn(III) porphyrin to Mn(II)porphyrin is a one-electron reduction and may lead to the formation of a Rh(II) species (eq 19).

$$[Mn(III)]^+ + [Rh(I)] \rightarrow [Mn(II)] + [Rh(II)]^+ \quad (19)$$

$$2\,[Rh(II)]^+ \rightarrow [Rh(I)] + [Rh(III)]^{2+} \quad (20)$$

$$[Mn(III)]^+ + [Rh(II)]^+ \rightarrow [Mn(II)] + [Rh(III)]^{2+} \quad (21)$$

These Rh(II) species are known to disproportionate very fast to give a Rh(I) and a Rh(III) complex (eq 20). Second-order rate constants of this reaction have been reported to be as large as $10^9\ M^{-1}s^{-1}$.[33] Another possibility is that the Rh(II) species reacts with a second manganese porphyrin (eq 21). In view of a possible application of our rhodium complexes in a Cytochrome P_{450} mimic the latter reactions should be supressed since efficient activation of dioxygen by Mn(III)porphyrin requires a fast but limited supply of only two electrons (one for the reduction of Mn(III) to Mn(II) and one for the reaction: $Mn(II) + O_2 + 2H^+ \rightleftharpoons Mn^V{=}O + H_2O$).[6] The use of polymerized bilayer systems with covalently anchored rhodium complexes could be very promising in this regard. Further studies are under way.

Experimental Section

General Methods. ^{1}H-NMR spectra were recorded on a Bruker WH 90 instrument (90 MHz). Chemical shifts are given in ppm downfield from tetramethylsilane. Abbreviations used are s = singlet, d = doublet, t = triplet, m = multiplet, b = broad. Transmission electron microscopy was carried out with an Philips EM 201 instrument. A Branson 2200 sonication bath was used for the preparation of the vesicles by the sonication method. Infrared and UV–vis spectra were recorded on Perkin-Elmer 298 and Perkin-Elmer Lambda 5 spectrophotometers, respectively. The cuvettes for UV–vis measurements were thermostated with an accuracy of 0.1 °C. Electrochemical measurements were made using a PAR Model 173 potentiostat equipped with a PAR Model 176 I/E converter, coupled to a PAR Model 175 universal programmer.

Materials. Technical grade solvents were used, unless otherwise indicated. DMF and THF were distilled before use. Column chromatography and TLC were performed on silica (Merck, silica gel 60H and precoated F-254 plates, respectively). For the preparation of the vesicles Uvasol grade solvents (Merck) and deionized and triple distilled water were used. The compounds 5,10,15,20-tetrakis((4-hexadecyloxy)-phenyl)porphyrin,[5] (((2-pyridyl)carbonyl)methyl)pyridinium iodide,[40] tetrakis(4-sulfonatophenyl)porphyrin manganese(III)[41] (mnTSPP), and *N*-hexadecyl-*N*-(11-hydroxyundecyl)-*N*,*N*-dimethylammonium chloride[42] were synthesized according to literature procedures. $[RhCp^*Cl_2]_2$ was prepared from hexamethyldewarbenzene and rhodium(III) trichloride.[43] 10-Methylalloxazine (Fl) was a gift from the Laboratory of Organic Chemistry, University of Wageningen, The Netherlands.

***N*-Hexadecyl-*N*-(11-(methacryloxy)undecyl)-*N*,*N*-dimethylammonium Chloride (MHACl).** Pyridine (2 mL) and 2.65 g of freshly destilled methacryloyl chloride (0.0254 mol) was slowly added to a solution of 8.48 g of *N*-hexadecyl-*N*-(11-hydroxyundecyl)-*N*,*N*-dimethylammonium chloride (0.015 mol) in 40 mL of dichloromethane at 0 °C. The reaction mixture was allowed to warm to room temperature. After the mixture was stirred for 16 h, the solvent was removed at reduced pressure. The oily residue was purified by column chromatography (silica, eluent 7 vol % of methanol in dichloromethane): 5.38 g of a white waxy product (0.0085 mol, 57%); ^{1}H-NMR ($CDCl_3$) δ 6.1 (m, 1H), 5.5 (m, 1H), 4.2 (t, 2H), 3.5 (br m, 10H), 1.9 (s, 3H), 2.0–1.0 (br m, 46H), 0.9 (t, 3H); IR (neat) ν/cm^{-1} 1715, 1630.

5-Methyl-2,2′-bipyridine (1). A mixture of 6.5 g (0.02 mol) of (((2-pyridyl)carbonyl)methyl)pyridinium iodide, 40 mL of formamide, and 40 g of ammonium acetate was heated at 60 °C with stirring. After the compounds had been dissolved completely, 2.25 mL of methacrolein (0.038 mol) was added. Stirring was continued for 4 h at 60 °C and subsequently for 16 h at room temperature. The product was isolated from the reaction mixture by extraction with diethyl ether (3 × 100 mL). The diethyl ether layers were combined and washed with 100 mL of a 1 wt % aqueous sodium carbonate solution, dried (Na_2SO_4), and concentrated under vacuum: 3.0 g of a brown oil (0.0187 mol, 93%); single spot on TLC, $R_f = 0.4$ (silica, eluent 5 vol % methanol in chloroform); ^{1}H-NMR ($CDCl_3$) δ 8.62 (d, 1H), 8.48 (s, 1H), 8.30 (m, 2H), 7.78 (t, 1H), 7.61 (d, 1H), 7.26 (t, 1H), 2.37 (s, 3H).

2,2′-Bipyridine-5-carboxylic Acid (2). A solution of 3.0 g (0.0187 mol) of 5-methyl-2,2′-bipyridine and 10 g of potassium permanganate in 125 mL of water was boiled until the purple color had disappeared. The progress of the reaction was followed by taking from time to time an aliquot (0.5 mL) of the solution, extracting it with diethyl ether (1 mL), and analyzing it by TLC. If necessary, 2.5 g of potassium permanganate was carefully added to the reaction mixture and boiling was continued. After all 5-methyl-2,2′-bipyridine had reacted the reaction mixture was cooled to room temperature and filtered. The filtrate was acidified to pH = 1 by adding concentrated HCl and subsequently concentrated under vacuum to approximately 30 mL. The product that precipitated was collected on a glass filter. After the filtrate stood for 2 days in a refrigerator a second portion had crystallized out and was then collected on a glass filter. The fractions were combined and dried under vacuum: 2.1 g (0.011 mol, 59%) of a white crystalline powder; ^{1}H-NMR (DMSO-d_6) δ 9.13 (s, 1H), 8.73 (d, 1H), 8.44 (m, 3H), 8.11 (t, 1H), 7.62 (m, 1H), 5.5 (b); IR (KBr) ν/cm^{-1} 3050 (b s), 1730 (s).

2,2′-Bipyridine-5-*N*-(6-hydroxyhexyl)carboxamide (4). 2,2′-Bipyridine-5-carboxylic acid (0.5 g, 2.6 mmol) was added to 25 mL of thionyl chloride and refluxed for 16 h. The thionyl chloride was removed under vacuum. The yellow reaction product was dissolved in 5 mL of dichloromethane and added to a solution of 2.0 g (0.017 mol) 6-aminohexanol in 25 mL of dichloromethane. A few crystals of 4-(*N*,*N*-dimethylamino)-pyridine were added, and the solution was stirred for 20 h. The reaction mixture was concentrated under vacuum and purified by column chromatography (silica, eluent 5 vol % of methanol in chloroform): 0.40 g (1.33 mmol, 51%) of a white powder; ^{1}H-NMR ($CDCl_3$) δ 9.04 (s, 1H), 8.71 (m, 1H), 8.47 (m, 2H), 8.19 (m, 1H), 7.84 (m, 1H), 7.34 (m, 1H), 6.3 (b, 1H), 3.57 (m, 4H), 1.8–1.2 (b m, 8H); IR (neat) ν/cm^{-1} 3400 (b m), 3290 (m), 1630 (s), 1540 (s).

2,2′-Bipyridine-5-*N*-(11-hyroxyundecyl)carboxamide (5). This compound was synthesized as described for 2,2′-bipyridine-5-*N*-(6-hydroxyhexyl)carboxamide, starting from 0.5 g (2.6 mmol) of 2,2′-bipyridine-5-carboxylic acid and 2.0 g (0.011 mol) of 11-aminoundecanol: yield 0.51 g (1.38 mmol, 52.5%) of a white powder; ^{1}H-NMR ($CDCl_3$) δ 9.03 (s, 1H), 8.71 (d, 1H), 8.50 (m, 1H), 8.46 (m, 1H), 8.19 (m, 1H), 7.84 (m, 1H), 7.36 (m, 1H), 6.23 (t, 1H), 3.5 (m, 4H), 1.8–1.1 (br m, 18H).

2,2′-Bipyridine-5-*N*-(6-(methacryloxy)hexyl)carboxamide (6). Methacryloyl chloride (2.0 mL, 0.018 mol) was slowly added to a solution of 0.4 g (1.34 mmol) of 2,2′-bipyridine-5-*N*-(6-hydroxyhexyl)carboxamide in 10 mL of chloroform and 5 mL of pyridine. After the mixture was stirred at room temperature for 16 h, 100 mL of chloroform was added. The reaction mixture was extracted with aqueous 1 N HCl (2 × 75 mL) and 75 mL of a saturated aqueous sodium carbonate solution, dried (Na_2SO_4), and concentrated under vacuum. The

(40) Krohnke, F.; Gross, K. F. *Chem. Ber.* **1959**, *93*, 33.
(41) Fleisher, E.; Palmer, J. M.; Srivastava, T. R.; Chatterjee, A. *J. Am. Chem. Soc.* **1971**, *93*, 3162–3167.
(42) Roks, M. F. M. Ph.D. Thesis, University of Utrecht, The Netherlands, 1987.
(43) Kang, J. W.; Moseley, K.; Maitles, P. M. *J. Am. Chem. Soc.* **1969**, *91*, 5970–5977.

crude product was purified by column chromatography (silica, eluent 3 vol % of methanol in dichloromethane): yield 0.315 g (0.86 mmol, 64%) of a white powder; ^{1}H-NMR ($CDCl_3$) δ 9.04 (s, 1H), 8.71 (d, 1H), 8.50 (m, 1H), 8.46 (m, 1H), 8.20 (m, 1H), 7.84 (m, 1H), 7.37 (m, 1H), 6.38 (t, 1H), 6.11 (s, 1H), 5.56 (s, 1H), 4.19 (t, 2H), 3.51 (m, 2H), 1.96 (s, 3H), 1.8–1.1 (br m, 8H); IR (neat) ν/cm^{-1} 3300 (m), 1710 (s), 1630 (s), 1540 (m, NH). Anal. Calcd for $C_{21}H_{25}N_3O_3$: C, 68.64; H, 6.68; N, 11.44. Found: C, 67.95; H, 6.84; N, 11.06.

2,2′-Bipyridine-5-*N*-(11-(methacryloxy)undecyl)carboxamide (7). This product was synthesized as described for 2,2′-bipyridine-5-*N*-(6-(methacryloxy)hexyl)carboxamide, starting from 0.470 g (1.27 mmol) of 2,2′-bipyridine-5-*N*-(11-hydroxyundecyl)carboxamide and 2.0 mL (18 mmol) of methacryloyl chloride: yield 0.325 g (0.74 mmol, 58%) of a white powder; ^{1}H-NMR ($CDCl_3$) δ 9.03 (s, 1H), 8.71 (d, 1H), 8.50 (m, 1H), 8.46 (m, 1H), 8.19 (m, 1H), 7.84 (m, 1H), 7.36 (m, 1H), 6.16 (t, 1H), 6.10 (s, 1H), 5.54 (s, 1H), 4.14 (t, 2H), 3.5 (m, 2H), 1.96 (s, 3H), 1.8–1.1 (br m, 18H). Anal. Calcd for $C_{26}H_{35}N_3O_3$: C, 71.37; H, 8.06; N, 9.60. Found: C, 71.01; H, 8.11; N, 9.52.

***N*-(2-(2-Aminoethoxy)ethyl)-*N*,*N*-dihexadecyl-*N*-methylammonium Chloride (8).** A solution of 1.5 g (2.4 mmol) of *N*-(2-(2-chloroethoxy)ethyl)-*N*,*N*-dihexadecyl-*N*-methylammonium chloride and 0.5 g of sodium azide in 50 mL of acetone was refluxed for 16 h. The reaction mixture was concentrated under vacuum, dissolved in 50 mL of dichloromethane, and extracted with a aqueous 0.1 N HCl solution. The organic layer was dried (Na_2SO_4) and concentrated under reduced pressure. The resulting white solid was dissolved in 30 mL of THF and cooled to 0 °C. Lithium aluminum hydride (0.5 g) was added over an period of 10 min with stirring. After the mixture was stirred for 30 min at 0 °C, 5 mL of a saturated aqueous ammonium chloride solution was carefully added. After gas evolution had ceased, 50 mL of an aqueous 2 N HCl solution was added, and the mixture was extracted three times with 50 mL of dichloromethane. The organic layers were combined, washed with aqueous 1 N sodium hydroxide solution, dried (Na_2SO_4), and concentrated under vacuum to give a white solid product: yield 1.3 g (2.15 mmol, 91%); ^{1}H-NMR ($CDCl_3$) δ 3.9 (b s, 6H), 3.5–3.2 (m, 7H), 2.85 (t, 2H), 1.8–1.3 (m, 56H), 0.9 (t, 6H); IR (neat)ν/cm^{-1}: 3360 (s), 1073 (s).

***N*-(2-(2-(2,2′-Bipyridine-5-carboxamido)ethoxy)ethyl)-*N*,*N*-dihexadecyl-*N*-methylammonium Chloride (9).** This compound was synthesized as described for 2,2′-bipyridine-5-*N*-(6-hydroxyhexyl)carboxamide, starting from 0.5 g (2.6 mmol) of 2,2′-bipyridine-5-carboxylic acid (0.0026 mol) and 1.3 g (2.15 mmol) of *N*-(2-(2-aminoethoxy)ethyl)-*N*,*N*-dihexadecyl-*N*-methylammonium chloride. After purification by column chromatography (silica, eluent 10 vol % of methanol in dichloromethane) a white solid product was obtained: yield 0.95 g (0.12 mmol, 56%) of a white powder; ^{1}H-NMR ($CDCl_3$) δ 9.43 (s, 1H), 9.24 (b, 1H), 8.67 (m, 1H), 8.40 (m, 2H), 7.84 (m, 1H), 7.30 (m, 1H), 4.2–3.6 (b m, 8H), 3.5–3.2 (m, 7H), 1.8–1.3 (m, 56H), 0.9 (t, 6H); IR (neat) ν/cm^{-1} 3400 (w), 3230 (m), 1650 (s), 1546 (w), 1079 (m). Anal. Calcd for $C_{48}H_{85}N_4O_2Cl$: C, 73.38, H, 10.91; N, 7.13. Found: C, 73.19; H, 11.07; N, 6.96.

(2,2′-Bipyridine-5-(*N*-(6-(methacryloxy)hexyl)carboxamide)(pentamethylcyclopentadienyl)rhodium Dichloride (RhC_6). To a suspension of 0.093 g (0.3 mmol of $[RhCp^*Cl_2]_2$ in 2.5 mL of methanol was added 0.106 g (0.29 mmol) of 2,2′-bipyridine-5-*N*-(6-(methacryloxy)hexyl)carboxamide. Within 30 s a clear orange solution was formed. The reaction mixture was stirred for 30 min, filtered over a glass filter, and concentrated under vacuum to give an orange oil. The product was precipitated by adding 10 mL of diethyl ether and subsequently stirring for 24 h (when necessary the suspension was sonicated in a bath-type sonicator for 30 min at room temperature): yield 0.16 g (82%) of a yellow hygroscopic powder; ^{1}H-nmr ($CDCl_3$) δ 10.04 (b t, 1H), 9.42 (b, 2H), 8.96 (b, 1H), 8.13 (b, 2H), 7.82 (b, 2H), 6.09 (s, 1H), 5.51 (s, 1H), 4.11 (t, 2H), 3.53 (br m, 2H), 1.93 (s, 3H), 1.71 (s, 15H), 1.3 (b, 8H). Anal. Calcd for $C_{31}H_{40}Cl_2N_3O_3Rh{\cdot}H_2O$: C, 53.67; H, 6.11; N, 6.06. Found: C, 53.22; H, 6.13; N, 5.89.

(2,2′-Bipyridyl-5-(*N*-(11-(methacryloxy)undecyl)carboxamide)(pentamethylcyclopentadienyl)rhodium Dichloride (RhC_{11}). This compound was synthesized as described for RhC_6, starting from 0.160 g (0.37 mmol) of 2,2′-bipyridine-5-*N*-(11-(methacryloxy)undecyl)carboxamide and 0.114 g (0.185 mmol) of $[RhCp^*Cl_2]_2$: yield 0.255 g (92%) of a yellow hygroscopic powder; ^{1}H-NMR ($CDCl_3$) δ 10.0 (b, 1H), 9.40 (b, 2H), 8.98 (b, 1H), 8.20 (b, 2H), 7.87 (b, 2H), 6.10 (s, 1H), 5.56 (s, 1H), 4.02 (t, 2H), 3.53 (br m, 2H), 1.90 (s, 3H), 1.67 (s, 15H), 1.3 (b, 18H). Anal. Calcd. for $C_{36}H_{50}Cl_2N_3O_3Rh{\cdot}1.5H_2O$: C, 55.89; H, 6.91; N, 5.43. Found: C, 55.78; H, 6.82; N, 5.34.

(*N*-(2-(2-(2,2′-Bipyridyl-5-carboxamido)ethoxy)ethyl)-*N*,*N*-dihexadecyl-*N*-methylammonium)(pentamethylcyclopentadienyl)rhodium Trichloride (RhN). This compound was synthesized as described for RhC_6, starting from 0.314 g (0.40 mmol) of *N*-(2-(2-(2,2′-bipyridine-5-carboxamido)-ethoxy)ethyl)-*N*,*N*-dihexadecyl-*N*-methylammonium chloride and 0.124 g (0.20 mmol) of $[RhCp^*Cl_2]_2$: yield 0.415 g (94%) of a yellow powder; ^{1}H-NMR ($CDCl_3$) δ 10.4 (b, 1H), 9.6 (b d, 1H), 9.4 (s, 1H), 8.95 (b d, 1H), 8.5 (b d, 2H), 8.2 (b t, 1H), 7.9 (b t, 1H), 4.2–3.2 (b m, 15H), 1.8–1.3 (m, 56H), 0.9 (t, 6H), and 2.1 (s, ~9H). Anal. Calcd for $C_{55}H_{100}Cl_3N_4O_2Rh{\cdot}5H_2O$: C, 58.80; H, 9.36; N, 4.73. Found: C, 59.05; H, 9.42; N, 4.69.

***N*-Octyl-2-chloroacetamide.**[44] 2-Chloroacetyl chloride (16.7 g, 0.081 mol) and 0.1 g of *N*,*N*-dimethyl-4-aminopyridine were dissolved in 50 mL of dichloromethane and cooled to 0 °C. Octylamine (12.9 g, 0.1 mol) and 10 mL of triethylamine were added in 1 h with stirring. The reaction mixture was stirred for another hour after which the resulting precipitate was filtered off. The filtrate was extracted with 1 N aqueous HCl, dried ($MgSO_4$), and evaporated to dryness. The oily residue was distilled: yield 12.3 g (60%) of a waxy product; bp 119–120 °C (0.25 Torr); ^{1}H-NMR ($CDCl_3$) δ 6.9 (b s, 1H), 4.1 (s, 2H), 3.35 (q, 2H), 1.3 (b m, 12H), 0.9 (t, 3H).

***N*-Dodecyl-2-chloroacetamide.** This compound was synthesized as described for *N*-octyl-2-chloroacetamide, starting from 9.3 g (0.05 mol) of dodecylamine and 5 g (0.044 mol) of 2-chloroacetyl chloride. After evaporation of the solvent the crude product was recrystallized from diethyl ether: yield 6.2 g (0.024 mol, 54%) of a waxy product; ^{1}H-NMR ($CDCl_3$) δ 6.6 (b s, 1H), 4.1 (s, 2H), 3.35 (q, 2H), 1.3 (b m, 20H), 0.9 (t, 3H).

***N*-Hexadecyl-2-chloroacetamide.** This compound was synthesized as described for *N*-octyl-2-chloroacetamide, starting from 11 g (0.046 mol) of hexadecylamine and 5 g (0.044 mol) of 2-chloroacetyl chloride. After evaporation of the solvent the crude product was recrystallized from diethyl ether: yield 6.5 g (0.021 mol, 47%) of a waxy product; ^{1}H-NMR ($CDCl_3$) δ 6.5 (b s, 1H), 4.1 (s, 2H), 3.35 (q, 2H), 1.3 (b m, 28H), 0.9 (t, 3H).

1-(*N*-Octylcarbamoyl)methyl-3-carboxamidopyridinium Chloride (C_8NA^+). 3-Pyridinecarboxamide (3.0 g, 0.025 mol) and 6.0 g (0.029 mmol) of *N*-octyl-2-chloroacetamide were dissolved in acetone and refluxed for 24 h. After the reaction mixture was cooled to room temperature, the resulting crude product was filtered off, washed with acetone, and recrystallized three times from acetone–acetonitrile (1/1 v/v): yield 1.35 g (17%) of pale yellow crystals; ^{1}H-NMR ($CDCl_3$ + drop of CD_3OD) δ 11.3 (s 0.5H), 9.55 (s, 1H), 9.05 (m 2H), 8.7 (s, 0.25H), 8.20 (m, 1H), 5.5 (s, 2H) 3.25 (t, 2H), 1.3 (b m, 12H), 0.9 (t, 3H); UV–vis (H_2O) λ_{max}/nm (ϵ/M^{-1}·cm^{-1}) 267 (4300).

1-(*N*-Dodecylcarbamoyl)methyl-3-carboxamidopyridinium Chloride ($C_{12}NA^+$). This compound was synthesized as described for (C_8NA^+, starting from 1.22 g (0.01 mol) of 3-pyridinecarboxamide and 3.0 g (0.0115 mol) of *N*-dodecyl-2-chloroacetamide. Recrystallization from ethanol (three times) gave 2.0 g (54%) of pale yellow crystals: ^{1}H-NMR ($CDCl_3/CD_3OD$ ~ 4/1) δ 11.45 (s, 1H), 9.51 (s, 1H), 9.0 (m, 2H), 8.7 (s, 0.25H), 8.21 (m, 1H), 5.6 (s, 2H), 3.23 (t, 2H), 1.3 (b m, 20H), 0.9 (t, 3H); UV–vis (H_2O) λ_{max}/nm (ϵ/M^{-1}·cm^{-1}) 267 (4180).

1-((*N*-Hexadecyl)carbamoyl)methyl)-3-carboxamidopyridinium Chloride ($C_{16}NA^+$). This compound was synthesized as described for C_8NA^+, starting from 1.22 g (0.01 mol) of 3-pyridinecarboxamide and 3.9 g (0.0112 mol) of *N*-hexadecyl-2-chloroacetamide. Recrystallization from etha-

(44) Hornibrook, W. J.; Janz, G. J.; Gordon, A. R. *J. Am. Chem. Soc.* **1947**, *64*, 515–516.

nol (three times) gave 2.1 g (48%) of pale yellow crystals: ^{1}H-NMR ($CDCl_3/CD_3OD$ ~ 3/1) δ 11.45 (s, 1H), 9.55 (s, 1H), 9.01 (m, 2H), 8.7 (s, 0.5H), 8.20 (m, 1H), 5.55 (s, 2H), 3.21 (t, 2H), 1.3 (b m, 28H), 0.9 (t, 3H); UV–vis (H_2O) λ_{max}/nm (ϵ/M^{-1}·cm^{-1}) 267 (4100).

5,10,15,20-Tetrakis(4-(hexadecyloxy)phenyl)porphyrinmanganese(III) Chloride. This compound was synthesized as described in the literature for 5,10,15–20-tetraphenylporphyrinmanganese(III) chloride,[45] starting from 0.4 g (0.25 mmol) of 5,10,15,20-tetrakis(4-(hexadecyloxy)phenyl)porphyrin and 1 g of manganese(II) acetate: yield 410 mg (96%) of a dark powder; UV–vis (CH_2Cl_2, λ_{max}/nm (ϵ/M^{-1}·cm^{-1})) 356 (4.43), 380 (4.60), 408 (4.57), 479 (4.86), 584 (3.82), 624 (4.01).

Preparation of the Catalysts. Incorporation of RhC_6 and RhC_{11}. A dispersion of 62.4 mg (0.1 mmol) of MHACl in 2.0 mL of water was sonicated in a bath-type sonicator for 1 h at 40 °C. An amount of the rhodium complex (10^{-6}–10^{-5} mol) was added to this optically clear solution, and the solution was vortexed until the rhodium complex had dissolved.

Incorporation of RhN. In a test tube 11 mg of RhN (10^{-5} mol) was added to a solution of 63 mg (0.1 mmol) of MHACl in 0.5 mL of CH_2Cl_2. The solvent was evaporated under a stream of nitrogen to leave a homogeneous mixed film of the rhodium complex and the surfactant. The sample was dried for 2 h in a vacuum desiccator at 0.2 mmHg. Water (preheated at 50 °C) was added to the mixed film while vortexing. The resulting dispersion was placed in a bath-type sonicator and sonicated for 1 h at 40 °C.

Incorporation of MnTHPP. In a test tube of 0.42 mL of a 1.2 mM stock solution of MnTHPP in CH_2Cl_2 (0.5×10^{-6} mol) was added to a solution of 157 mg (0.25 mmol) of MHACl in 0.5 mL of CH_2Cl_2. The solvent was evaporated under a stream of nitrogen to leave a homogeneous mixed film of the porphyrin and the surfactant. The sample was dried for 1 h under vacuum. For samples prepared by the sonication method 5 mL of water (preheated at 50 °C) was added to the mixed film while vortexing. The resulting dispersion was placed in a bath-type sonicator and sonicated for 2 h at 50 °C. For samples prepared by the ethanol injection method the mixed film was solubilized in 1 mL of ethanol/THF (1/2 v/v). This solution was injected into the vortex of 50 mL of rapidly stirred water (~1000 rpm, preheated at 50 °C). Finally, this solution was concentrated to a volume of 5 mL by ultrafiltration in a 50 mL Amicon cell equipped with a YM 100 membrane.

Incorporation of MnTHPP, RhC_{11}, and RhN. In case of RhC_{11} an amount of the rhodium complex was added to an aqueous dispersion MnTHPP and MHACl which was prepared as described above. For catalyst solutions that contained both MnTHPP and RhN, the latter compound was added to the CH_2Cl_2 solution before preparation of the mixed film.

Polymerization. A 0.02 mL aliquot of a 0.12 M solution of AIBN (2.5×10^{-6} mol) in ethanol was added to an aqueous dispersion of the rhodium complex and MHACl (1 mL, prepared as described above) while vortexing. The solution was carefully degassed, placed under argon, and polymerized for 2 h at 70 °C. Water (50 mL) was added, and the free rhodium complex that was left was removed by ultrafiltration (Amicon YM 100 membrane). The latter procedure was repeated (typically 4–5 times) until the concentration of the rhodium complex in the filtrate was below its detection limit (UV–vis). Finally, the volume of the residue was adjusted to 10 mL and the concentration of the rhodium complex was determined by UV–vis. The concentrations of the rhodium complexes varied per catalyst preparation. Their concentrations in the reaction mixtures are given for each experiment in the Results.

Ion Exchange. A polymerized solution of the catalyst (10 mL, 5 mM of MHACl) was placed on a column packed with an ion-exchange resin (1 × 20 cm, DOWEX 1-X2, bromide form) and eluted with water. The fractions containing the rhodium catalyst were combined and concentrated by ultrafiltration (Amicon YM 100 membrane) to a volume of 10 mL. The fraction of rhodium that was recovered was better than 95% of the initial concentration, as was checked by UV–vis.

Cyclic Voltammetry. For the measurements in water we used a basal cleaved pyrolytic graphite electrode as the working electrode together with a platinum auxiliary electrode. The graphite electrode was polished with alumina, rinsed with water and cleaned in a bath-type sonicator for 1 min before use. In dichloromethane platinum working and auxiliary electrodes were used. The reference electrode was a SSCE, separated by a salt bridge of similar composition and pH (but without the redox active compound) from the sample compartment. The measurements in dichloromethane were carried out in a glovebox, using freshly prepared solutions of the rhodium complexes. For the electrochemical measurements in water dispersions of the catalysts were used which were prepared as described above. In a typical measurement 1 mL of the catalyst and 3 mL of the buffer were placed in the electrochemical cell and purged with argon for 20 min. Prior to the measurements cyclic voltamograms were recorded between 0 and −0.8 V with a scan rate of 50 mV·s^{-1} until a stable signal was obtained. This typically required 30 min.

Kinetic Measurements. For the kinetic measurements an aqueous buffer of 50 mM *N*-ethylmorpholine/formic acid of pH 6.9 was used. In a typical experiment 1.9 mL of a solution of the buffer, sodium formate, and the substrate was placed in a quartz cuvette and degassed by bubbling argon through the solution for 15 min. The cuvette was immediately closed with a rubber septum and placed in the thermostated cuvette holder of the spectrophotometer. The temperature was left to equilibrate for 15 min, and 0.1 mL of a degassed solution of the catalyst was added with the help of a microsyringe. The course of the reaction was followed by measuring the change of the absorbance (λ/nm (log $\Delta\epsilon$)): Fl 431 (3.97); NA^+, C_8NA^+, $C_{12}NA^+$, and $C_{16}NA^+$ 267 (3.63); MnTSPP 466 (4.92); MnTHPP 440 (4.60).

Experiments at Various pH Values. An aliquot (10 mL) of an aqueous solution of 50 mM *N*-ethylmorpholine and 350 mM formic acid was adjusted to the desired pH value with a concentrated sodium hydroxide solution. The resulting solution was used as the buffer solution in the experiments, which were carried out as described above. The formation of the rhodium(I) complex was followed by the increase of the absorbance at 520 nm (T = 37.5 °C). After 5–15 min, a constant value of the absorbance was obtained which was used as the equilibrium value A_{pH}. The pH curve was obtained by plotting $(A_{pH}-A_{pH,min})/(A_{pH,max}-A_{pH,min})$ against the pH. $A_{pH,min}$ and $A_{pH,max}$ are the values of the absorbance at ~2 pH units below and ~2 pH units above the pK_a, respectively.

Acknowledgment. This work was supported by the Netherlands Foundation for Chemical Research (SON), with financial aid from the Netherlands Organization for Scientific Research (NWO).

Supplementary Material Available: Complete proton NMR data (31 pages). This material is contained in libraries of microfiches, immediately follows the article in the microfiche version of the journal, and can be ordered from the ACS; see any current masthead page for ordering information.

JO9405516

(45) van der Made, A. Ph.D Thesis, University of Utrecht, The Netherlands, 1988.